ACS OMEGA

Open Access

http://pubs.acs.org/journal/acsodf

Article

Modified Sanliangsan Improved Sjogren's Syndrome Complicated with Interstitial Lung Disease by Suppressing Serum MUC1 Levels

Lihui Tan, Wang Lv, Yuqi Chen, Jianjian Dong, Dun Mao, and Rong Wei*

Cite This: *ACS Omega* 2024, 9, 30392−30403

Read Online

ACCESS | Metrics & More | Article Recommendations | Supporting Information

ABSTRACT: Objectives: To clarify if the mechanism of Sanliangsan in improving Sjogren's syndrome complicated with interstitial lung disease (SS-ILD) involves MUC1 suppression, which is involved in SS-ILD pathogenesis. Methods: Fifty-six patients were randomly divided into two groups receiving Sanliangsan prescription (SP) therapy and conventional therapy (western medicine). In-depth transcriptome profiles from a large database of SS-ILD patients were collected and analyzed to identify candidate genes involved in SS pathogenesis. Clinical symptom scores, metabolic compositions, lung HRCT (high-resolution computed tomography) scores, and serum MUC1 levels were compared between the two groups before and after treatment. Network pharmacology, molecular docking, and ITC assays were performed to identify bioactive compounds of SP in improving SS. Metabolome analyzed the metabolic composition of serum associated with SS-ILD before and after SP treatment. Results: Transcriptome results identified the involvement of abnormal expression of genes relevant to the immune system, inflammatory responses, and signaling pathways. Numerous genes, including *CD58*, *CD86*, *CTLA4*, *CXCL8*, *STAT1*, and especially *MUC1*, were involved in SS pathogenesis and could be used to diagnose SS-ILD early. Both treatments improved the lung HRCT scores and clinical symptoms of SS-ILD. The SP therapy improved SS-ILD more effectively than conventional therapy. Moreover, Sanliangsan prescription therapy reduced serum MUC1 levels and restored the abnormal metabolisms, improving the abnormal inflammatory and immune responses of patients. Eugenol directly interacted with MUC1, suppressed related genes, and was the bioactive compound of SP. SP could partially restore the abnormal metabolisms associated with SS-ILD pathogenesis. Conclusion: Based on conventional Western medicine treatment, modified Sanliangsan can significantly improve the clinical symptoms, signs, and lung function of patients; the mechanism may be due to eugenol and related to MUC1 regulation.

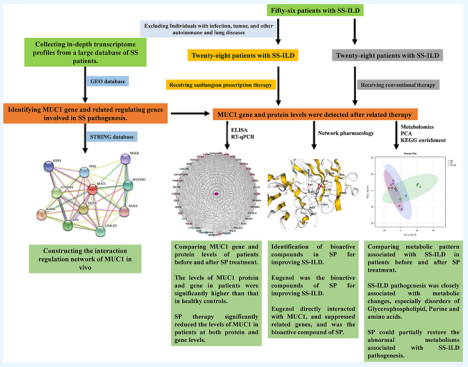

INTRODUCTION

Sjogren's syndrome (SS) is an autoimmune exocrine disease, mainly involving lacrimal and salivary glands and other exocrine glands.[1] This disease, characterized by dry lips and eyes, typically affects middle-aged women. Sjogren's syndrome mostly affected female groups, and the patient ages ranged from 45 to 55 years old.[2] It often involves multiple organs in development, especially the lungs. Up to 40% of clinically diagnosed cases of SS experience deleterious symptoms related to the blood, lungs, and urinary system, which can profoundly affect patients' quality of life.[3] Due to SS, B lymphocytes with hyperfunction infiltrate the exocrine gland, leading to the destruction of tissue structure.[4] Due to the large blood vessel network and connective tissues in the lung, about 11.4% of patients are complicated with interstitial lung disease (ILD),[5] and the probability of significant lung damage is 9−24%.[6] Patients with SS complicated with ILD (SS-ILD) have a 4-fold higher risk of death.[5] As a result, establishing strategies for early diagnosis and effective therapy is critical for treating such diseases. Currently, many researchers are trying to investigate the potential genes involved in the pathogenesis of SS to develop clinical indicators and drug targets that contribute to implementing effective early intervention strategies. Previous studies documented the involvement of pro-inflammatory cytokines, amplification of T cells, and cellular super mutation of B cells in SS pathogenesis.[7−9] The secretion of cytokines related to innate immunity induced the inflammatory hyperactivity observed during SS.[10] Thus, the dysregulation of cytokines associated with abnormal immune activation is one of the main causes of SS.[11−13] Recent studies showed that serum salivary glycochain antigen (MUC1) could be used as a biomarker of ILD in connective tissue diseases (CTD-ILD), and its level can reflect the damage to alveolar epithelium and stroma, which is of great significance in evaluating the disease and improving the prognosis.[14] Numerous studies showed the high expression of *MUC1* in the tissue of patients with SS,[15,16]

Received: February 18, 2024
Revised: June 17, 2024
Accepted: June 27, 2024
Published: July 5, 2024

implying that *MUC1* may be potentially involved in SS-ILD pathogenesis. However, the detailed role of *MUC1* in patients with SS-ILD is unclear.

In combination with antifibrosis medicines, glucocorticoids and immunosuppressants are commonly used to treat patients with SS-ILD in Western medicine. However, the price of these drugs that inhibit pulmonary fibrosis is high for most patients. Statistically, the global price of antifibrosis drugs in 2017 was as high as $348 million,[17] limiting their usage in the clinic. Interestingly, various studies have shown that traditional Chinese medicine could improve clinical symptoms of SS and reduce the toxic effects of Western drugs, playing an important role in improving prognosis and living standards.[18] The Sanliangsan prescription derived from a folk secret test recipe, and has been utilized for improving numerous diseases in clinic.[19−21] Its fundamental composition consists of Astragalus, honeysuckle, angelica, licorice, and centipede.[19,20] Previous research found that Sanliangsan could improve the symptoms of pneumonia via suppressing the expression of *TGF-β1*, with less adverse reactions in clinic.[19,20] In the present study, in-depth transcriptome profiles of the salivary gland, parotid, and peripheral blood from many patients were analyzed to identify potential targets involved in the pathogenesis of SS-ILD. Then, the effect and underlying mechanism of Sanliangsan prescription in improving SS-ILD were elucidated. We found that Sanliangsan prescription could suppress MUC1 and its related regulation network, while metabolome profiles suggested that SP could restore the abnormal metabolisms associated with SS-ILD. Importantly, numerous bioactive compounds from Sanliangsan were identified to improve SS-ILD, especially eugenol could directly interact with MUC1 and suppressed related genes to improve the symptoms of patients with SS-ILD.

MATERIALS AND METHODS

Samples Information. Fifty-six patients with SS-ILD who were admitted to the People's Hospital of Suzhou New District from June 10, 2018, to June 10, 2020, and met the international classification (diagnostic) criteria of SS-ILD were selected. Individuals with infection, tumor, and other autoimmune and lung diseases were excluded. The study was supported by Suzhou Science and Technology Development Project (SKJYD2021188). Signed informed consent was obtained from all participants. Considering that the primary age of the patient ranged from 45 to 55 years,[2] 28 healthy physical examination subjects matched in age and gender during the same period were selected as the control group for conventional therapy (CK) (age 52.68 ± 1.37 years). Another 28 patients were selected for Sanliangsan prescription (SP) (age 52.21 ± 1.36 years). There was no significant difference in age between the two groups (t = 1.196, P = 0.411). The control group received conventional treatment (hormone, antifibrosis drugs, oxygen therapy, immunosuppression); the SP group received Western medicine and conventional basic treatment combined with SP. SP was provided by the People's Hospital of Suzhou New District, one pair per day, which lasted for 90 days. The symptoms of cough and sputum, shortness of breath, and weakness were scored as 0, 3, 6, and 9 based on severity. Based on severity, the mouth and eye dryness were scored as 0, 1, 2, and 4. The high-resolution computed tomography (HRCT) of the lung was scored following the Fleischner guide. The range involved in each level of signs was scored as follows: no sign: 0.0; <5%: 1.0; 5−25%: 2.0; 25−50%: 3.0; 50−75%: 4.0; >75%: 5.0.

Data Collection and Expression Analysis. Keywords such as "Sjögren's syndrome", "salivary gland", "parotid", "peripheral blood", and "transcriptomics or microarray" were used in the GEO (Gene Expression Omnibus) database to find relevant transcriptome data sets of patients with SS. Finally, three data sets (GSE40611, GSE23117, GSE66795) with a large number of patients were collected to identify differentially expressed genes (DEGs) associated with SS. All data sets were processed using the Affymetrix array, and the Robust Multiarray Average method was applied to the data for background correction and normalization. Limma and DEseq2 R packages were used to identify the DEGs.[22] Fold change > 2.0 and adjusted P < 0.05 using the Benjamin Hochberg method were set as a cutoff to identify DEGs.

Functional Enrichment Analysis and Protein−Protein Interaction Network Construction. The gene ontology (GO) and pathway enrichment analyses were performed using the R package Clusterprofiler. The protein−protein interaction network was constructed using the String database. The degree, closeness, and betweenness were employed to assess the topology of this network. GO and pathway analysis terms were considered significant if the P value was lower than 0.05. The rich factors of each term were produced using the hypergeometric distribution method.

Determination of Serum MUC1 Levels by ELISA. Fasting elbow venous blood (3 mL) was extracted from the subjects in the morning, and the serum was routinely separated through 3000 rpm centrifugation. ELISA kit (purchased from Wuhan Boshide Biological Co., Ltd.) was used to detect the level of MUC1 in the serum according to the instructions mentioned on the kit.

RNA Extraction and RT-qPCR Assay. Total RNA of whole peripheral blood samples was extracted using a total RNA extraction kit (#AM1561, Ambion), following the manufacturer's instructions. Total RNA was used for reverse transcription to obtain cDNA using the PrimeScript RT Reagent kit (Takara). *MUC1* and *APP* expression levels were quantified via qPCR using a LightCycler 480 and SYBR Green I Master Mix (Roche). Expression levels were normalized to Actin (ACT) and were analyzed using the $2^{-\triangle\triangle CT}$ method. The average was used in statistical analyses, and assays were performed in duplicates.

Metabolomics Analysis Based on LC-MS/MS. Serum of SS-ILD before and after SP therapy was transferred to an EP tube. After the addition of 400 μL of extract solution (acetonitrile:methanol = 1:1, containing isotopically-labeled internal standard mixture), the samples were vortexed for 30 s and sonicated for 10 min in ice−water bath. Then, the sample was centrifuged at 12,000 rpm for 15 min. The supernatant was transferred to a fresh glass vial for analysis. LC-MS/MS analyses were performed using a UHPLC system (Vanquish, Thermo Fisher Scientific) with a UPLC BEH Amide column (2.1 mm × 100 mm, 1.7 mm) coupled to Q Exactive HFX mass spectrometer (Orbitrap MS, Thermo). The mobile phase consisted of 25 mmol/L ammonium acetate and 25 ammonia hydroxides in water (pH = 9.75) (A) and acetonitrile (B). The autosampler temperature was 4 °C, and the injection volume was 3 mL. The raw data were converted to the mzXML format using ProteoWizard and processed with an in-house program, which was developed using R and based on XCMS, for peak detection, extraction, alignment, and integration. Then, the

https://doi.org/10.1021/acsomega.4c01147
ACS Omega 2024, 9, 30392−30403

metabolites were identified using MS2 information. The cutoff for annotation was set at 0.3.

The analysis of data variation was performed by R packages XCMS software. The principal component analysis (PCA) and metabolite and pathway enrichment analysis were performed by Metaboanalyst 3.0. The data were further treated through mean centering and unit variance scaling. And the therapy $P < 0.05$ and fold change (FC) > 2 was used to identify significantly differential metabolites.

Statistical Methods. Statistical analyses were performed using SPSS Statistics 21.0 software. All data were quantitative, normally distributed by the Kolmogorov−Smirnov normality test, and expressed as mean ± standard deviation ($X \pm S$). The groups were tested using a two-sided t test or ANOVA for continuous variables and the Chi-squared statistics for categorical variables. A two-sided $P < 0.05$ was used to denote statistical significance.

Network Pharmacology and Molecular Docking Analyses. Network pharmacology analysis was performed following Ma et al.[23] The targets of related bioactive compounds were identified from the public PharmMapper Server databases (http://lilab.ecust.edu.cn/pharmapper/) based on similarities and pharmacophore models. We used LC-MS to identify the metabolites in Sanliangsan (Table S3) and used these metabolites for network pharmacology analysis. Then, the 100 protein conformations of related metabolites were identified as candidate targets of these metabolites.

Software AutoDock 4.2 was deployed to dock MUC1 and related bioactive compounds from Sanliangsan. Based on default values in AutoDock, we used ΔG to evaluate the binding affinity between MUC1 and related metabolites of Sanliangsan.

Protein Expression and Purification. The prokaryotic expression system of MUC1 was performed following Du et al.[24] The full coding sequencing of human MUC1 gene was ligated into the PGEX-4T vector for protein purification with GST-tag (Transheep Biotechnology, Shanghai, China). The positive 4T vector containing MUC1 was converted into BL21 (DE3), then isopropyl-D-thiogalactopyranoside (IPTG) was added to enhance MUC1 expression for 4 h at 37 °C. The recombinant MUC1 protein was obtained by GST-tag protein purification kit (Beyotime Biotechnology, Shanghai, China), then collected, and dialyzed in PBS glycerol buffer.

Isothermal Titration Calorimetry. Isothermal titration calorimetry assay for MUC1 and eugenol interaction was performed on an iTC200 (Nano ITC) following Du et al.[25] Eugenol (10 mM) was used as the ligand and titrated into the MUC1 protein solution (0.05 mM in PBS). The volume of each titration was set as 2.5 mL, while water was used as the negative control to eliminate the influence of background.

RESULTS

Improvement in the Condition of Patients with SS-ILD due to SP. The clinical characteristics of recruited patients with SS-ILD before and after treatments were documented and analyzed (Tables 1 and 2). The conventional therapy was set as the control group (CK). The clinical characteristics included cough and sputum, shortness of breath, weakness, HRCT scores, dry mouth, and dry eyes (Tables 1 and 2). There was no significant difference in the levels of these characteristics between CK and SP treatment groups (Tables 1 and 2). Both treatments effectively alleviated SS-ILD symptoms, and HRCT scores of patients were significantly decreased. The symptoms of cough and sputum, shortness of breath, weakness, dry mouth, and dry eyes were alleviated by both treatments (Tables 1 and 2). The symptoms in 26 patients were improved by SP treatment, whereas symptoms in only 18 patients were improved in the CK group, suggesting that SP treatment was more efficient than CK treatment (Table 1). The SP treatment improved cough and sputum, shortness of breath, weakness, dry mouth, and dry eyes in patients more significantly than CK treatment (Table 2). These results supported the notion that SP therapy could effectively improve SS-ILD more than conventional therapy.

Table 1. Effects of SP Therapy on Patients in the Clinic

variables	CK	SP	P value
healed case (n = 28)	18 (64.29%)	26 (92.86%)	0.009
HRCT (before treatment)	2.00 ± 0.72	2.04 ± 0.64	0.84
HRCT (after treatment)	1.71 ± 0.53*	1.54 ± 0.51*	0.20

*$P < 0.05$.

Transcriptomic Variations in the Peripheral Blood of Patients with SS. To investigate the detailed biological processes involved in SS-ILD pathogenesis and identify potential clinical index, we analyzed in-depth transcriptome profiles from many patients with SS. Transcriptome profiles of peripheral blood from 36 patients with severe SS were collected in the experimental group (SS; GSE66795), while profiles of 29 healthy individuals were used as controls (HT). After a data processing series, the $P < 0.05$ and Log2Foldchange were set as the threshold to identify DEGs. We obtained 919 genes that matched the threshold as differentially expressed genes (DEGs) by comparing gene expression profiles of the peripheral blood from patients with SS with those from normal healthy controls (Figure 1A). Among all DEGs, 456 genes were upregulated in SS vs HT, while the expression levels of 463 genes were downregulated in the peripheral blood of patients with SS (Figure 1A and Table S1).

To further investigate the biological processes associated with the pathogenesis of SS, we performed GO enrichment analysis on these 919 DEGs in SS vs HT comparison. The GO enrichment results showed that 8540 GO terms were identified against these DEGs, with 116 significant GO terms among the three main groups, including biological process, molecular function, and cellular component (FDR < 0.05; Table S2). Ten important terms relevant to molecular function were structural constituent of ribosome, protein binding, hydrolase activity, nucleoside monophosphate kinase activity, binding, hemoglobin binding, and chemokine receptor binding (Figure 1C and Table S2). Among cellular component categories, 33 terms were significantly altered in the peripheral blood of patients with severe SS, suggesting that these DEGs mainly functioned at the cytosolic ribosome, ribosome, cytoplasm, cytosol, intracellular, ribonucleoprotein complex, focal adhesion, cell-substrate adherens junction, hemoglobin complex, cell-substrate junction, extracellular organelle, extracellular vesicle, anchoring junction, and platelet α granules (Figure 1B and Table S2). We noted that focal adhesion and cell-substrate adherens junction were enriched in SS vs HT comparison, demonstrating its importance in SS pathogenesis (Figure 1B and Table S2). For biological processes, 71 categories were significantly identified, especially genes involved in myeloid cell and erythrocyte homeostasis, immune system process, hemopoiesis, immune system development, hematopoietic or

https://doi.org/10.1021/acsomega.4c01147
ACS Omega 2024, 9, 30392−30403

Table 2. Clinical Characteristics of Patients after Therapy ($X \pm S$)

group	time	cough and sputum	breath shortness	weakness	dry mouth and eye
SP	before	4.39 ± 1.73	3.96 ± 1.42	3.96 ± 1.43	2.57 ± 0.92
	after	2.25 ± 1.75$^{\#,*}$	3.00 ± 1.41$^{\#,*}$	3.11 ± 0.99$^{\#,*}$	2.07 ± 0.90$^{\#,*}$
CK	before	4.18 ± 1.70	3.75 ± 1.32	3.75 ± 1.32	2.71 ± 0.97
	after	3.64 ± 1.25$^{\#}$	3.21 ± 1.13$^{\#}$	3.21 ± 1.13$^{\#}$	2.43 ± 0.96$^{\#}$

$^{\#}P < 0.05$ vs before. $^{*}P < 0.05$ vs CK.

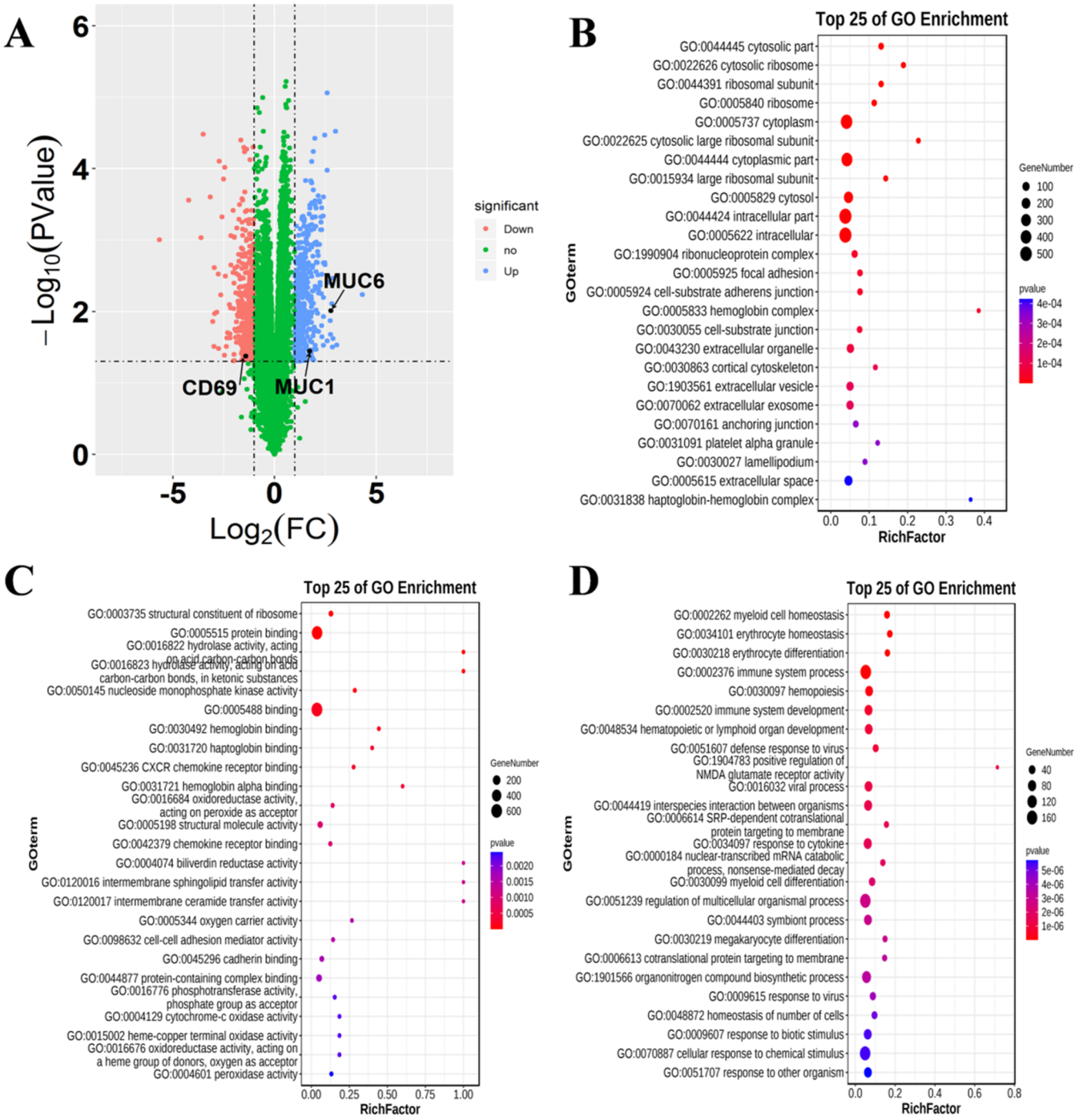

Figure 1. Landscape of transcriptome patterns in peripheral blood of patients with SS. (A) Volcano plots display the DEGs in SS vs HT comparison. Upregulated and downregulated genes are shown in red and blue, respectively. (B−D) Scatter plots of GO enrichment results of DEGs in SS vs HT comparison: (B) cellular component; (C) molecular function; (D) biological progress. The size and color represent the gene number and significance of each GO term.

https://doi.org/10.1021/acsomega.4c01147
ACS Omega 2024, 9, 30392−30403

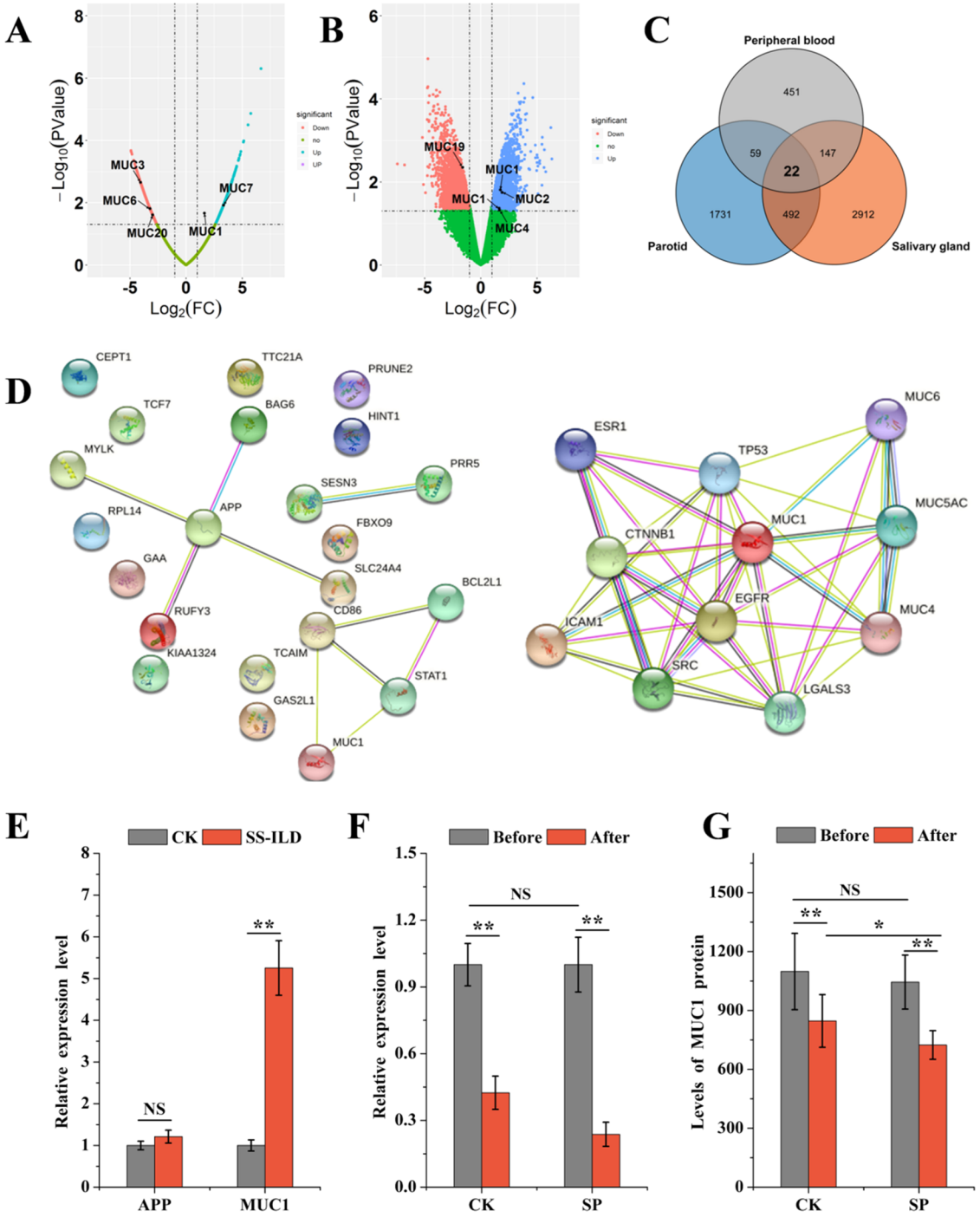

Figure 2. SP treatment suppresses hub SS-related MUC1 expression to improve SS-ILD. (A, B) Volcano plots display the DEGs in the salivary gland (A) and parotid (B) of patients with SS. The hub genes associated with SS are labeled by a black arrow. (C) Venn diagram displays the hub DEGs shared in the salivary gland, peripheral blood, and parotid of patients with SS. The DEGs from the salivary gland, peripheral blood, and parotid are represented by orange, gray, and blue circles, respectively. (D) Topological protein−protein interaction network of hub DEGs associated with SS. (E) Relative expression levels of *APP* and *MUC1* in patients with SS-ILD vs healthy individuals. (F) Expression level of *MUC1* in serum of patients with SS-ILD before and after SP and CK treatments. (G) ELISA of the serum protein levels of MUC1 in patients with SS-ILD before and after SP and CK treatments; "NS: no significance; *$P < 0.05$; **$P < 0.01$".

lymphoid organ development response to cytokine (Figure 1D and Table S2). These results suggested that variations in genes relevant to the immune system, cytokines, and focal adhesion may be involved in the pathogenesis of SS.

Possible Improvement in SS-ILD after Sanliangsan Treatment by Suppressing MUC1 Essential in the SS Pathogenesis. Two transcriptome profiles (GSE40611 and GSE23117) of the parotid and salivary glands from patients with SS were collected to identify the potential SS pathogenesis targets. In total, 3169 and 6025 genes were identified as DEGs in the parotid and salivary glands of patients with SS, respectively (Figure 2A,B). We noted that 22 DEGs were shared in these three transcriptome profiles (Figure 2C). Typically, 11 genes exhibited the same expression patterns in

https://doi.org/10.1021/acsomega.4c01147
ACS Omega 2024, 9, 30392−30403

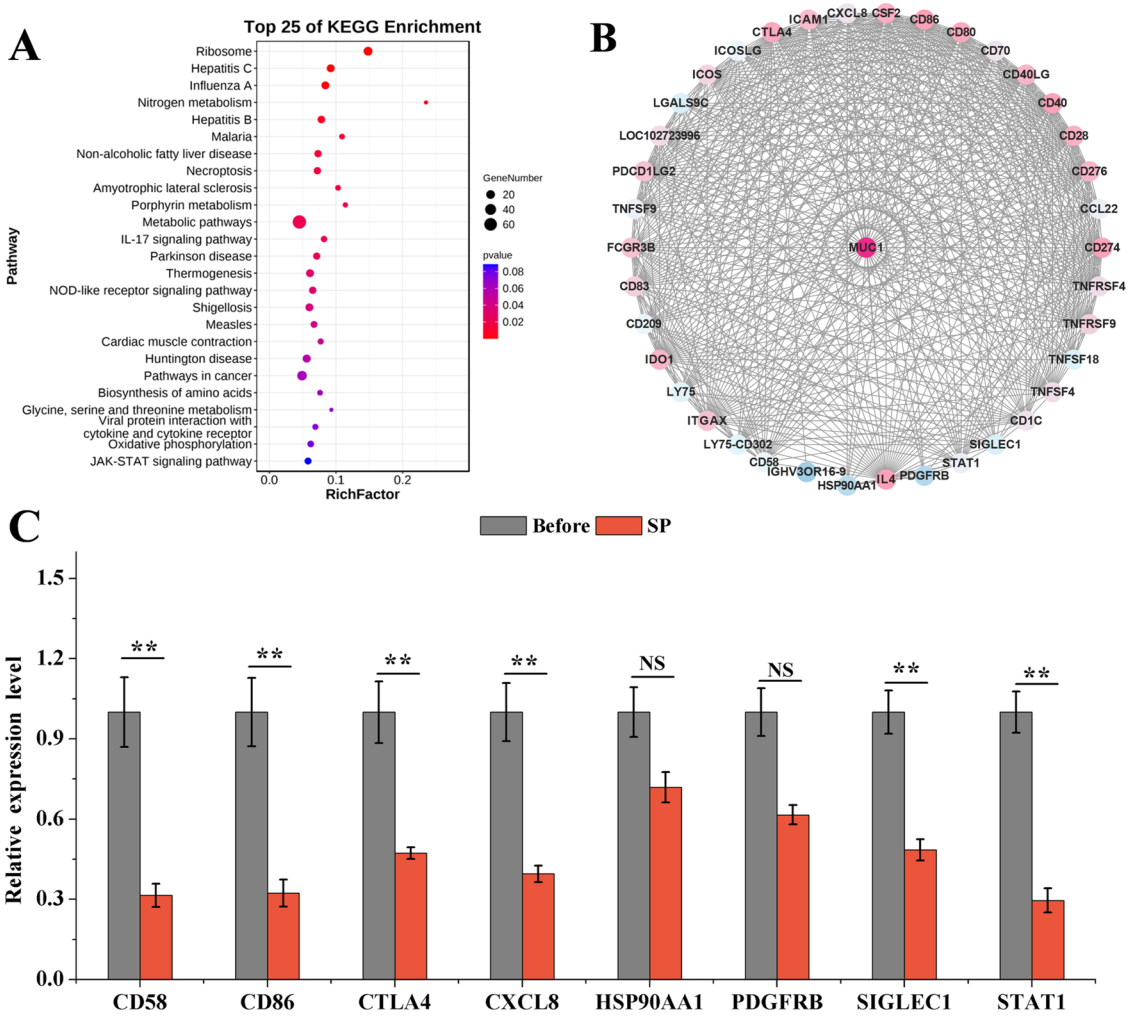

Figure 3. SP therapy improves SS-LID by affecting the regulation network of *MUC1*. (A) Scatter plot displays the pathway enrichment results of transcriptome profiles of the peripheral blood of patients with SS. The plot size and color represent the gene number and significance of each pathway. (B) Protein−protein interaction network showing the potential regulator of MUC1. (C) Expression of genes interacting with MUC1 in the serum of patients with SS-ILD after SP therapy.

these three tissues, including *RUFY3*, *CEPT1*, *TTC21A*, *BAG6*, *SLC24A4*, *KIAA1324*, *APP*, *GAA*, *CD86*, *GAS2L1*, and *MUC1* (Figure 2D and Table S1). Further protein−protein interaction network showed that MUC1 and APP might be the potential hub genes involved in SS-ILD pathogenesis (Figure 2D). Most of the genes involved in the interaction network of *MUC1* were DEGs in the peripheral blood, parotid, and salivary glands of patients with SS (Figure 2D and Table S1). RT-qPCR results showed that the expression level of *MUC1* was significantly higher in the serum of patients with SS-ILD than in healthy individuals; however, patients with SS-ILD did not exhibit significant differences in the expression level of *APP* (Figure 2E). Thus, we proposed that *MUC1* was the potential hub gene involved in the pathogenesis of SS-ILD and could be used as a clinical indicator for SS-ILD detection. We further determined the protein and mRNA levels of MUC1 in the serum of patients with SS-ILD before and after treatment of SP using ELISA and RT-qPCR, respectively. The results showed that the expression level of *MUC1* was significantly suppressed in both CK and SP treatment groups. SP treatment could suppress *MUC1* expression more effectively than CK treatment (Figure 2F). ELISA results reached a consensus with RT-qPCR results and showed no significant difference in MUC1 levels among patients before CK and SP treatments (1098.57 ± 194.2 and 1044.64 ± 137.62 pg/mL; $t = 0.775$, $P = 0.454$; Figure 2G). Remarkably, the MUC1 level was significantly lower in the serum of patients with SS-ILD after SP treatment (724.29 ± 72.77) than in patients before SP treatment (Figure 2G). Moreover, the inhibitory effect of SP treatment on the MUC1 level was more significant than that of CK treatment. The MUC1 level in SS-ILD serum after CK treatment was 846.79 ± 134.13 pg/mL (Figure 2G). Together, these lines of evidence suggest that the MUC1 level contributed to SS-ILD pathogenesis, and SP treatment could suppress the MUC1 to improve SS-ILD more effectively than CK treatment.

Sanliangsan Treatment Suppressed Genes Associated with *MUC1* for Potentially Improving SS-ILD. Pathway enrichment analysis was performed on the DEGs from transcriptome profiles of the peripheral blood of patients with SS based on the Kyoto Encyclopedia of Genes and Genomes (KEGG) database. These 919 DEGs were enriched in 281 pathways, with 18 significant pathways (Figure 3A; $P < 0.05$). We noted various pathways relevant to the immune system and signal transduction were enriched in the peripheral blood of patients with SS, including cytokine-cytokine receptor interaction and signaling pathways of IL-17, NOD-like

https://doi.org/10.1021/acsomega.4c01147
ACS Omega 2024, 9, 30392−30403

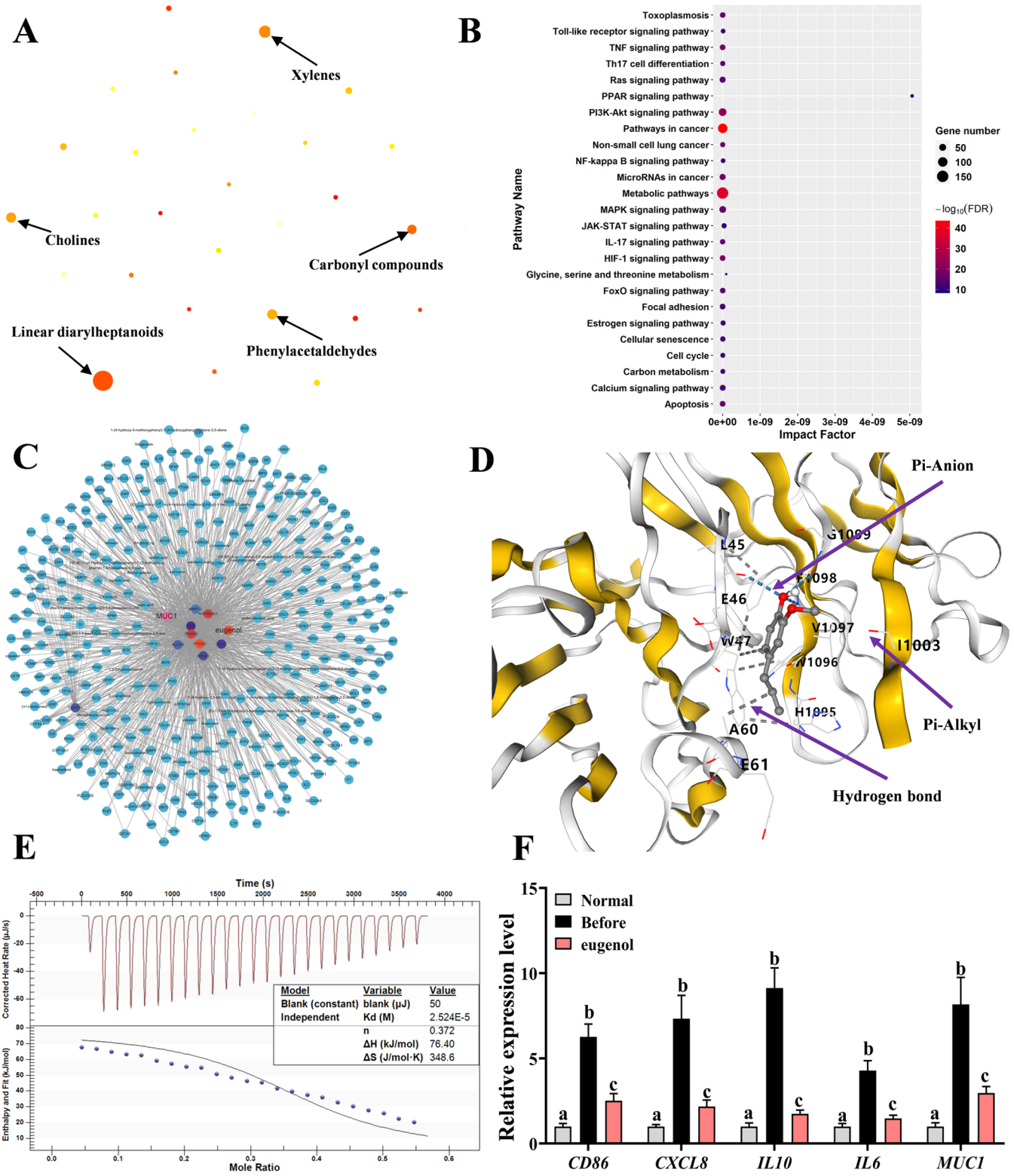

Figure 4. Network pharmacology analysis of SP in improving SS-ILD. (A) Category of metabolites from SP. (B) KEGG pathways analysis on targets of bioactive compounds of SP. (C) Integrated network of bioactive compounds and related proteins. (D) Molecular docking analysis detects the interaction between MUC1 protein and eugenol. (E) Isothermal titration calorimetry (ITC) enthalpograms of eugenol binding to MUC1. Titration data are presented as blue plots and fit as a black solid line. (F) RT-qPCR determines the effects of eugenol in affecting abnormal upregulation of genes involved in SS-ILD pathogenesis.

receptor, JAK-STAT, toll-like receptor, chemokine, and TNF (Figure 3A). Additionally, numerous pathways relevant to cell growth and death were also active in the peripheral blood of patients with SS, including apoptosis, cell cycle, p53 signaling pathway, cellular senescence, ferroptosis, and necroptosis (Figure 3A). These results suggested the involvement of these related pathways in SS pathogenesis. Considering the involvement of MUC1 in SS pathogenesis, we further

https://doi.org/10.1021/acsomega.4c01147
ACS Omega 2024, 9, 30392−30403

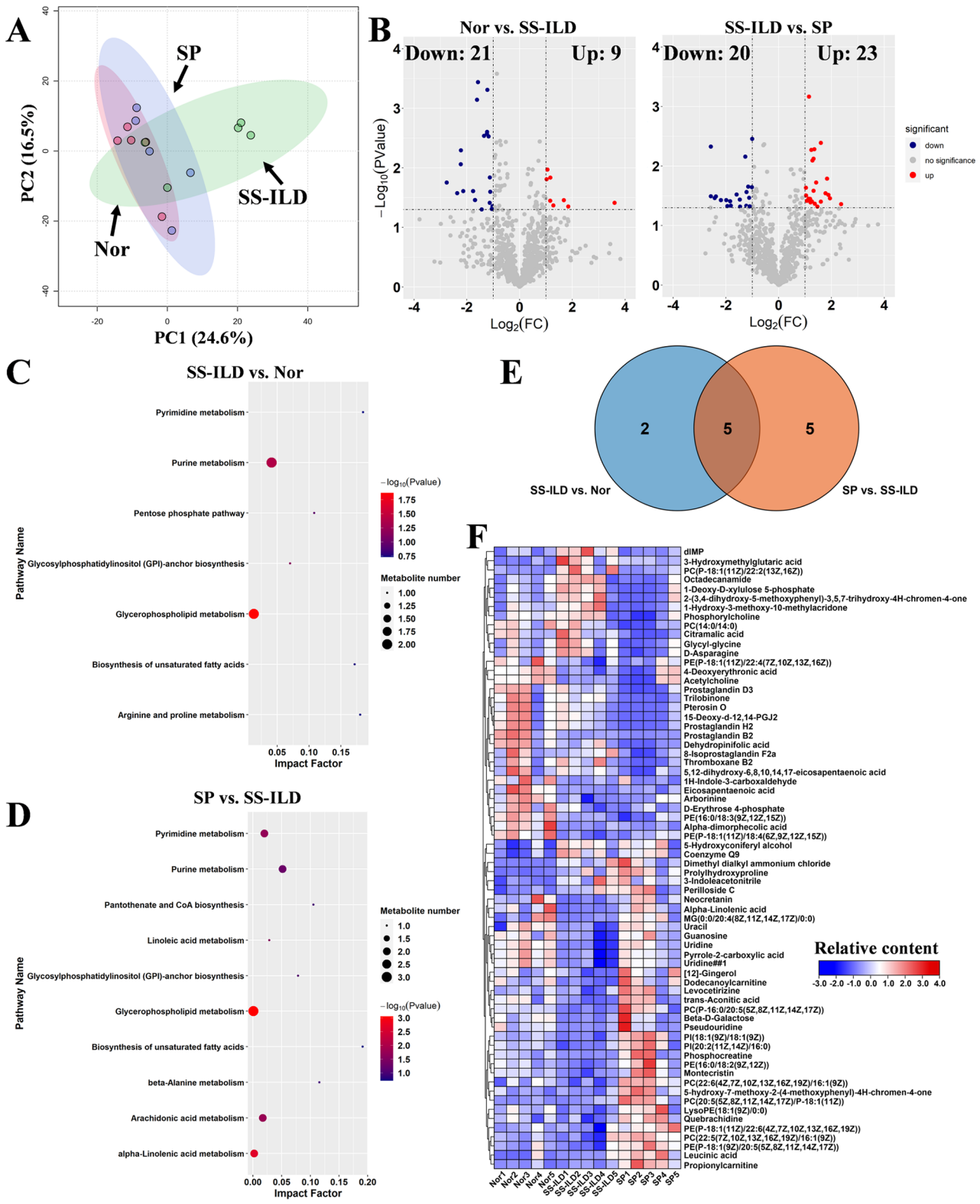

Figure 5. Metabolic variation in SS-ILD before and after SP treatment. (A) Principal component analysis (PCA) displays the separation of all groups and stability of biological replicates. The circles labeled by same color were the samples with the same treatment. PC1 and PC2 explain 24.6% and 10.5% of variances, and are used to construct the PCA plot based on the integral metabolomic profiles. (B) Volcano plots display the DEMs in SS-ILD vs Nor and SP vs SS-ILD comparisons based on $P < 0.05$ and fold change >2.0. (C, D) Scatter plot displaying the pathway enrichment results based on the differential metabolites in SS-ILD vs Nor and SP vs SS-ILD comparisons. The various color levels displayed different levels of significance of metabolic pathways from low (blue) to high (red). (E) Venn diagrams show the overlapping of pathways between SS-ILD vs Nor and SP vs SS-ILD comparisons. (F) Heat map displaying the relative contents of metabolites associated with the pathogenesis of SS-ILD and SP. The scale represents the normalized peak area of metabolites in each biological replicates.

https://doi.org/10.1021/acsomega.4c01147
ACS Omega 2024, 9, 30392−30403

constructed the interaction network of *MUC1* and genes involved in these pathways (Figure 3B). The topological network displayed complex regulation relationships among these genes; especially *MUC1* performed important roles in the network (Figure 3B). Additionally, eight genes that interacted with *MUC1* were identified in the network, including *CD58*, *CD86*, *CTLA4*, *CXCL8*, *HSP90AA1*, *PDGFRB*, *SIGLEC1*, and *STAT1* (Figure 3B). Numerous studies have shown that the upregulation of these genes is involved in the pathogenesis of SS.[7−9,14] Importantly, SP therapy effectively suppressed the upregulation of most of these genes in the serum of patients with SS-ILD, including *CD58*, *CD86*, *CTLA4*, *CXCL8*, *SIGLEC1*, and *STAT1* (Figure 3C), which may further result in the dysregulation of *MUC1* and improve SS-ILD.

Network Pharmacology Identified the Bioactive Compounds of SP That Improved SS-ILD. To investigate the bioactive compounds of SP in improving SS-ILD, we detected the metabolic compositions of SP using LC-MS. Totally, 556 metabolites were identified in SP (Table S3). These metabolites mainly belonged to Isoprenoids, prenol lipids, hydrocarbons, fatty acids and conjugates, benzoic acids, flavonoids, cinnamic acids, linear diarylheptanoids, fatty alcohols and carbonyl compounds (Figure 4A). Then, we performed network pharmacology analysis on these 556 metabolites using TCMSP online tools (Traditional Chinese Medicine Systems Pharmacology Database and Analysis Platform) to identify the bioactive compounds of SP in improving SS-ILD. The TCMSP results identified 45 bioactive metabolites in SP, including eugenol, Terpineol, linalool, 1,2-Dihydrocurcumin, Curcumin, Sitogluside, vanillic acid, β-selinene, 1,8-cineole, copaene, farnesol, oleic acid, protocatechuic acid, rutin, kaempferol, quercetin, and coumarin (Table S4). Totally, 600 proteins were identified as candidate targets of these 556 compounds in SP (Table S4). Then, we analyzed the function of these targeted proteins using GO and KEGG enrichment algorithm. Go enrichment analysis on these 600 targets showed that these targets mainly performed their functions in extracellular space, cytoplasm, extracellular region, vesicle, extracellular exosome, extracellular vesicle, intracellular organelle lumen, plasma membrane region, secretory granule, and membrane raft (Table S5). These targets exhibited activities of identical protein binding, catalytic activity, enzyme binding, ion binding, small-molecule binding, anion binding, oxidoreductase activity, and vitamin binding (Table S5) and response to oxygen compound, response to chemical, response to nitrogen compound, small-molecule metabolic process, regulation of multicellular organismal process, response to lipid, positive regulation of cellular process, and metabolic process (Table S5). KEGG pathway enrichment analysis on these 600 targets showed the significant enrichment of pathways in cancer, metabolic pathways, PI3K-Akt signaling pathway, HIF-1 signaling pathway, MicroRNAs in cancer, TNF signaling pathway, IL-17 signaling pathway, and MAPK signaling pathway (Figure 4B). Further disease enrichment analysis showed that these targets are involved in various diseases, including breast cancer, cancer, viral infections, ulcerative colitis, and especially Sjogren's syndrome (Table S4), supporting the involvement of SP in affecting SS-ILD. Typically, numerous pathways relevant to MUC1 were identified as targets of compounds from SP, implying that SP could improve SS-ILD via targeting MUC1.

Finally, we integrated these results in the topological network to identify the hub bioactive compounds of SP in improving SS-ILD. The results showed that these targets formed a complex network, and eugenol was the hub compound that was involved in the mechanisms of SP in improving UC (Figure 4C). Importantly, compounds protocatechuic acid, eugenol, rutin, kaempferol, salicylic acid, kaempferol, acetic acid, rutin, kaempferol, coumarin, and quercetin targeted the proteins (arachidonate 5-lipoxygenase and thioredoxin reductase, cytoplasmic) involved in the pathogenesis of SS-ILD, of note eugenol also targeted MUC1 in the network (Figure 4C). Further molecular docking showed that eugenol could insert into the hydrophobic pocket of MUC1 with a credible score (ΔG = −8.5 kcal/mol; Figure 4D). Then, we determined the binding affinity between MUC1 and eugenol using ITC assay. The results showed that eugenol directly interacted with the MUC1 recombinant protein, with dissociation constants of K_{d1} = 25.2 μM (Figure 4E). Typically, the interaction between MUC1 and eugenol was caused by entropy-driven adsorption and endothermic processes ($\Delta H > 0$ & $\Delta S > 0$) (Figure 4E). Importantly, ITC assay reached a consensus with docking results that eugenol directly interacted with MUC1 through hydrophobic interactions (Figure 4D,E). Moreover, eugenol effectively attenuated the abnormal upregulation of *CD86*, *IL6*, *IL10*, *CXCL8*, and *MUC1* in the model mouse with Sjogren's syndrome (Figure 4F). Meanwhile, we further analyzed the binding affinity of MUC1 with other 16 bioactive compounds from Sanliangsan using molecular docking. Based on $\Delta G < -7.0$ kcal/mol, the docking results showed that 6 compounds of 16 bioactive chemicals from Sanliangsan also could interact with MUC1, including sitogluside, rutin, quercetin, kaempferol, 1,2-dihydrocurcumin, and curcumin (Figure S1 and Table S6). Typically, the top 3 most active compounds in interacting with MCU1 were sitogluside, eugenol, and rutin, with ΔG = −9.1, −8.5, and −8.7 kcal/mol, respectively (Figure S1 and Table S6). Overall, our network pharmacology analysis about SP suggested that eugenol was the bioactive compound of SP in improving SS-ILD via targeting MUC1.

Metabolic Landscape in Serum Associated with SS-ILD before and after SP Treatment. Our previous results showed that SS-ILD and *MUC1* were associated with numerous metabolisms. Here, we further investigate the metabolic changes in SS-ILD individuals before and after SP treatment. Totally, five biological replicates of serum from each group (SS-ILD and SP) were collected for metabolomics, and normal individuals were used as control (Nor) (Figure 5A). Principal component analysis (PCA) was performed on all metabolic profiles to global metabolic variations of rats from each group. The two-dimensional results showed that the samples were observably distributed into four regions according to their metabolic compositions (Figure 5A). The principal components 1 and 2 explained 24.6% and 16.5%, and most variations were generated between SS-ILD vs Nor and SP vs SS-ILD comparisons (Figure 5A). PCA results suggested that SS-ILD pathogenesis was closely associated with metabolic changes, whereas SP improved the abnormal metabolic changes in serum with SS-ILD (Figure 5A). Then, we used $P < 0.05$ and fold change > 2.0 to identify differentially expressed metabolites (DEMs). Totally, 30 (21 downregulated and 9 upregulated) and 43 (20 downregulated and 23 upregulated) DEMs were identified in SS-ILD vs Nor and SP vs SS-ILD comparisons, respectively (Figure 5B). OPLSDA analysis on SS-ILD vs Nor comparison showed that top 10 metabolites with the value of variable important in projection

https://doi.org/10.1021/acsomega.4c01147
ACS Omega 2024, 9, 30392−30403

(VIP) > 1.0 were inosine, pyrrole-2-carboxylic acid, uridine, arborinine, hypoxanthine, inosine, PC(18:3(6Z,9Z,12Z)/15:0), PC(20:3(8Z,11Z,14Z)/14:0), PE(P-18:1(11Z)/18:4-(6Z,9Z,12Z,15Z)), and 3-hydroxycapric acid; thus, these metabolites could be used as clinical indicators for SS-ILD diagnosis. Further pathway enrichment analysis on 30 DEMs from SS-ILD vs Nor showed that these metabolites involved in 7 pathways, including glycerophospholipid metabolism, purine metabolism, glycosylphosphatidylinositol (GPI)-anchor biosynthesis, pentose phosphate pathway, biosynthesis of unsaturated fatty acids, arginine and proline metabolism, and pyrimidine metabolism (Figure 5C). Similarly, DEMs from SP vs SS-ILD were also involved in these pathways and five related pathways from SS-ILD vs Nor were also enriched in SP vs SS-ILD (Figure 5C−E), suggesting that SP could affect the abnormal metabolisms associated with SS-ILD pathogenesis. Among these DEMs from both SS-ILD vs Nor and SP vs SS-ILD comparisons, we found that the SP performed opposite effect on their levels compared to SS-ILD. The metabolites that triggered to increase in SS-ILD were decreased by SP treatment, whereas most metabolites that decreased in SS-ILD were increased by SP treatment in vivo (Figure 5F). Taken together, these results suggested that SP could partially restore the abnormal metabolisms associated with SS-ILD pathogenesis.

DISCUSSION

SS-ILD is a systemic pulmonary autoimmune disease with a specific predisposition for causing inflammation of the lung tissue and is closely associated with multiple factors.[1] Thus, elucidating the detailed pathogenesis of SS-ILD will contribute to the development of related therapy and early diagnosis. In our present study, we identified the abnormal expression of various genes possibly involved in the pathogenesis of SS-ILD by analyzing in-depth transcriptome profiles from many patients with SS, especially MUC1, which can be used as a clinical indicator for the early detection and diagnosis of SS-ILD. These SS-ILD-related genes are mainly involved in inflammatory responses, immune system, and signaling pathways, such as cytokine-cytokine receptor interaction and signaling pathways of IL-17, NOD-like receptor, JAK-STAT, toll-like receptor, chemokine, and TNF. Importantly, we provided considerable evidence to show that the Sanliangsan treatment effectively improved patients' symptoms and lung HRCT scores. Although conventional therapy also improved SS-ILD symptoms, the effect of SP on SS-ILD was more effective. Furthermore, we found that SP mainly improved SS-ILD by reducing the abnormal MUC1 level in patients. At the same time, expression levels of various genes that interacted with MUC1 were also affected by SP therapy, improving patient survival. Importantly, we identified eugenol as the hub bioactive compound of SP in improving SS-ILD. Eugenol directly interacted with MUC1 and suppressed the expressions of genes relevant to SS-ILD pathogenesis, especially MUC1. Meanwhile, we identified that numerous other bioactive compounds from Sanliangsan also could target MUC1, including sitogluside, rutin, quercetin, kaempferol, 1,2-dihydrocurcumin, and curcumin. Additionally, metabolic profiles suggested that SP therapy effectively improved the abnormal metabolisms associated with the SS-ILD pathogenesis, especially glycerophospholipid metabolism, purine metabolism, glycosylphosphatidylinositol (GPI)-anchor biosynthesis, biosynthesis of unsaturated fatty acids, and pyrimidine metabolism. Our present study contributes to the understanding of SS-ILD pathogenesis. It also elucidates the underlying mechanism of SP in improving SS-ILD, contributing to the use of SP in improving SS-ILD in the clinic.

SS is an autoimmune disease that mainly affects the exocrine glands and lungs. It is characterized by cell infiltration, resulting in impaired organ function.[1] SS-related ILD is a major cause of disability and death in patients. Early diagnosis and understanding of the detailed pathogenesis of SS-ILD are essential for the effective therapy of this disease. The dysregulation of cytokines secreted by different cell subsets is the main cause of SS, while immune disorders also contribute to the onset and continuation of SS.[11,12] Secretion of cytokines could trigger abnormal autoimmune responses by promoting the survival of B cells and T cells and protecting T cells from apoptosis, leading to glandular damage in patients with SS.[13] We also found that genes relevant to cytokines and immune responses were highly expressed in the serum of patients with SS-ILD, suggesting their extensive involvement in different types of SS. We found that genes relevant to signaling pathways of IL-17, NOD-like receptor, STAT, chemokine, and TNF were also abnormally expressed in the serum of patients with SS-ILD. Importantly, previous studies have shown that these signaling pathways are involved in SS pathogenesis and host immune responses.[26] TNF-α and transforming growth factor (TGF-1) can induce the proliferation, differentiation, and collagen production of fibroblasts and promote the destruction of the basement membrane and the migration of fibroblasts by activating proteolytic enzymes, thus participating in the pathogenesis of ILD.[27] Therefore, genes involved in these pathways and responses could be used as potential clinical indicators for the early diagnosis of SS-ILD, including CD58, CD86, CTLA4, CXCL8, SIGLEC1, and STAT1. The involvement of these genes in host immune and inflammatory responses has been documented to be related to various diseases, especially SS.[28−30] We also identified that upregulation of MUC1 was the main characteristic of patients with SS-ILD. Thus, MUC1 can be used as a biomarker for patients with SS-ILD. MUC1 is a glycoprotein secreted mainly by type II alveolar epithelial cells and bronchial mucosal epithelial cells and acts as an important marker of pulmonary fibrosis and disease severity.[31] MUC1 expression is significantly increased in rheumatoid arthritis, pSS, dermatomyositis, and other connective tissue disease-related lung interstitial lesions.[32] We found that the serum MUC1 level > 500 U/mL suggested the existence of ILD, and when the serum KL-6 level is >1000 U/mL, ILD is in the active stage. This is of great significance in evaluating such diseases and improving the prognosis. Currently, the conventional therapy for SS-ILD includes hormones, biologics, immunosuppressants, and mesenchymal stem cell therapy. These therapies could improve lung function by inhibiting the immune-inflammatory response activated in patients with SS, reducing the infiltration of lymphocytes and plasma cells around alveolar epithelial cells and pulmonary capillaries, and reducing the inflammatory response, fibrinous exudation, and pulmonary tissue fibrosis.[33,34] However, these therapies were limited by their high price and insurance expense policies. Traditional Chinese medicine could effectively improve the condition of patients with SS-ILD without significant side effects.[18] We showed that SP therapy could improve symptoms and HRCT scores of patients with SS-ILD in the clinic. Its effect was more efficient than that of conventional therapy. The expression level of various genes is

https://doi.org/10.1021/acsomega.4c01147
ACS Omega 2024, 9, 30392−30403

involved in the pathogenesis of SS-ILD, especially MUC1. Moreover, the abnormal expression of multiple genes that interacted with MUC1 was also suppressed after SP therapy. These genes are mainly involved in inflammatory and immune responses. The function and abnormal expression of MUC1 have been observed in rheumatoid arthritis, pSS, dermatomyositis, and other connective tissue disease-related lung interstitial lesions.[14] Its abnormal expression will affect inflammatory responses by influencing TNF-α and NF-κB singling pathways[35,36] and promote tumor invasion and metastasis.[37,38] Thus, MUC1 was the potential target of SP therapy for improving the condition of patients with SS-ILD in the clinic and could be used as a clinical indicator for the early diagnosis of this disease.

In summary, our study elucidated that MUC1 contributes to SS-ILD pathogenesis by inducing inflammatory responses and immune-related signaling pathways. Importantly, MUC1 was the therapeutic target of SP therapy for effectively improving SS-ILD in the clinic. Numerous compounds were identified from Sanliangsan to involve in improving SS-ILD by targeting MUC1, including sitogluside, eugenol, rutin, quercetin, kaempferol, 1,2- dihydrocurcumin, and curcumin. Although eugenol was not the most active compound interacting with MUC1, we proved its binding affinity with MUC1, and the function of other bioactive chemicals in improving MUC1 will be our research focus in the future. Overall, our research provides the molecular basis for using SP in improving the condition of patients with SS-ILD in the clinic.

■ ASSOCIATED CONTENT

Data Availability Statement

The data underlying this study are available in the Supporting Information.

Supporting Information

The Supporting Information is available free of charge at https://pubs.acs.org/doi/10.1021/acsomega.4c01147.

Additional data (ZIP)

Transcriptome profiles of human with SS-ILD (Table S1); GO enrichment analysis on DEGs associated with the pathogenesis of SS-ILD (Table S2); identification of bioactive chemicals in Sanliangsan (Table S3); information of related targets of bioactive chemical of Sanliangsan in network pharmacology analysis (Table S4); GO enrichment analysis on proteins that identified as targets of bioactive chemical of Sanliangsan (Table S5); binding affinity between MUC1 and candidate bioactive compounds from Sanliangsan (Table S6); and interaction models of bioactive compounds with MUC1 protein (Figure S1) (PDF)

■ AUTHOR INFORMATION

Corresponding Author

Rong Wei − *Department of Rheumatology and Immunology, The People's Hospital of Suzhou New District, Suzhou 215000, China*; orcid.org/0009-0000-0203-7315; Email: sgyfsk@163.com

Authors

Lihui Tan − *Department of Rheumatology and Immunology, The People's Hospital of Suzhou New District, Suzhou 215000, China*

Wang Lv − *Department of Traditional Chinese Medicine, The Cangzhou central Hospital, Cangzhou 061000, China*

Yuqi Chen − *Department of Rheumatology and Immunology, The People's Hospital of Suzhou New District, Suzhou 215000, China*

Jianjian Dong − *Department of Rheumatology and Immunology, The People's Hospital of Suzhou New District, Suzhou 215000, China*

Dun Mao − *Department of Orthopaedic, Community Health Service Center of Suzhou Science and Technology City, Suzhou 215000, China*

Complete contact information is available at: https://pubs.acs.org/10.1021/acsomega.4c01147

Author Contributions

L.T. conceived and designed the experiments, performed the experiments, analyzed the data, prepared figures and/or tables, authored or reviewed drafts of the paper, and approved the final draft. Y.C. and W.L. performed the experiments, analyzed the data, prepared figures and/or tables, and approved the final draft. J.D. and D.M. performed the experiments, prepared figures and/or tables, and approved the final draft. R.W. conceived and designed the experiments, analyzed the data, prepared figures and/or tables, authored or reviewed drafts of the paper, and approved the final draft.

Notes

The authors declare no competing financial interest.

The People's Hospital of Suzhou New District granted Ethical approval to carry out the study within its facilities (Ethical Application Reference: 2018-012).

■ ACKNOWLEDGMENTS

The authors thank Dr. Youwei Du, Dr. Huiya Ma, and Dr. Hongchen Jia for providing English editing services and data analysis of this manuscript. They also thank Suzhou Science and Technology Development Project (SKJYD2021188) for its support.

■ REFERENCES

(1) Ganz, T.; Nemeth, E. Hepcidin and iron homeostasis. *Biochim. Biophys. Acta* **2012**, *1823* (9), 1434−1443.

(2) Kasper, D. L. *Harrison Department of Internal Medicine − Immunological and Rheumatic Diseases*, 19th ed.; Li, Z.et al., Translators; Peking University Medical Press: Beijing, 2016; pp 135−136.

(3) Velo-García, A.; Castro, S. G.; Isenberg, D. A. The diagnosis and management of thehaematologic manifestations of lupus. *J. Autoimmun.* **2016**, *74*, 139−160.

(4) Wu, R. H.; Ding, T. T.; Xue, H. W.; Li, X. F.; Wang, C. H. Research progress in the regulation of helper T cell 17/ regulatory T cell immune balance in rheumatoid arthritis by helper T cell 9/ interleukin-9. *J. Rheumatol.* **2020**, *24* (3), 206−209.

(5) Firestein, G. S.; Budd, R. C.; Gabriel, S. E.; McInnes, I. B.; O'Dell, J. R. *Kelley and Firestein's Textbook of Rheumatology*; Elsevier: Amsterdam, 2017.

(6) Palm, O.; Garen, T.; Enger, T. B.; Jensen, J. L.; Lund, M. B.; Aalokken, T. M.; Gran, J. T. Clinical pulmonary involvement in primary Sjogren's syndrome: Prevalence, quality of life and mortality – a retrospective study based on registry data. *Rheumatology* **2013**, *52* (1), 173−179.

(7) Nemeth, E.; Rivera, S.; Gabayan, V.; Keller, C.; Taudorf, S.; Pedersen, B. K.; Ganz, T. IL-6mediates hypoferremia of inflammation by inducing the synthesis of the ironregulatory hormone hepcidin. *J. Clin. Invest.* **2004**, *113* (9), 1271−1276.

(8) Zhou, D. L.; Chen, Y. T.; Chen, F. L.; Gallup, M.; Vijmasi, T.; Bahrami, A. F.; Noble, L. B.; van Rooijen, N.; McNamara, N. A. Critical involvement of macrophage in filtration in the development of Sjogren's syndrome-associated dryeye. *Am. J. Pathol.* **2012**, *181*, 753−760.
(9) Cong, X.; Zhang, X. M.; Zhang, Y.; Wei, T.; He, Q. H.; Zhang, L. W.; Hua, H.; Lee, S. W.; Park, K.; Yu, G. Y.; Wu, L. L. Disruption of endothelial barrierfunction is linked with hyposecretion and lymphocytic infiltration insalivary glands of Sjogren's syndrome. *Biochim. Biophys. Acta* **2018**, *1864*, 3154−3163.
(10) Bombardieri, M.; Barone, F.; Humby, F.; Kelly, S.; McGurk, M.; Morgan, P.; Challacombe, S.; De Vita, S.; Valesini, G.; Spencer, J.; Pitzalis, C. Activation-induced cytidinedeaminase expression in follicular dendritic cell networks andinterfollicular large B cells supports functionality of ectopic lymphoidneogenesis in autoimmune sialoadenitis and MALT lymphoma in Sjogren's syndrome. *J. Immunol.* **2007**, *179*, 4929−4938.
(11) Alunno, A.; Ibba-Manneschi, L.; Bistoni, O.; Rosa, I.; Caterbi, S.; Gerli, R.; Manetti, M. Mobilization of lymphaticendothelial precursor cells and lymphatic neovascularization in primary Sjogren's syndrome. *J. Cell. Mol. Med.* **2016**, *20*, 613−622.
(12) Holdgate, N.; St Clair, E. W. Recent advances in primary Sjogren's syndrome. *F1000Research* **2016**, *5*, 1412.
(13) Sun, Y. C.; Wang, Y.; Chen, S. J.; Fan, G. H.; Zhang, J. H.; Dai, F.; Qian, H. Y.; Liu, Y.; Shi, G. X. Expression of galphaq is decreased inlymphocytes from primary sjogren's syndrome patients and related toincreased IL-17A expression. *J. Immunol. Res.* **2018**, *2018*, No. 8212641.
(14) Fusconi, M.; Candelori, F.; Weiss, L.; Riccio, A.; Priori, R.; Businaro, R.; Mastromanno, L.; Musy, I.; de Vincentiis, M.; Greco, A. Qualitative mucin disorders in patients with primary Sjögren's syndrome: A literature review. *Med. Oral.* **2021**, *26* (1), e71−e77.
(15) Watanabe, H.; Maeda, N.; Kiritoshi, A.; Hamano, T.; Shimomura, Y.; Tano, Y. Expression of a mucin-like glycoprotein produced by ocular surface epithelium in normal and keratinized cells. *Am. J. Opthalmol.* **1997**, *124* (6), 751−757.
(16) Argüeso, P.; Balaram, M.; Spurr-Michaud, S.; Keutmann, H. T.; Dana, M. R.; Gipsoon, I. K. Decreased level of the goblet cell mucin MUC5AC in tears of patients with Sjögren syndrome. *Invest. Ophthalmol. Vis. Sci.* **2002**, *43* (4), 1004−1011.
(17) Miranda, H. F.; Sierralta, F.; Lux, S.; Troncoso, R.; Ciudad, N.; Zepeda, R.; Zanetta, P.; Noriega, V.; Prieto, J. C. Involvement of nitridergic and opioidergic pathways in the antinociception of gabapentin in the orofacial formalin test in mice. *Pharmacol. Rep.* **2015**, *67* (2), 399−403.
(18) Wei, S. J.; He, Q. M.; Zhang, Q.; Fu, K. H.; Li, R. L.; Peng, W.; Gao, Y. X. Traditional Chinese medicine is a useful and promising alternative strategy for treatment of Sjogren's syndrome: A review. *J. Integr. Med.* **2021**, *19* (3), 191−202.
(19) Lv, W.; Lihui, T.; Jiali, G.; Ying, W.; Qian, Y.; Xujie, Z.; Yang, Z. Clinical efficacy of Modified Sanliangsan combined western medicine on radioactive pneumonia. *China J. Trad. Chin. Med. Pharm.* **2019**, *34* (04), 1838−1840.
(20) Lv, W.; Lihui, T.; Jiali, G.; Ying, W.; Qian, Y.; Xujie, Z.; Yang, Z. Clinical study on treating leukopenia after radiotherapy with Sanliangsan. *China J. Trad. Chin. Med. Pharm.* **2019**, *11* (32), 115−118.
(21) Miao, J.; Peng, L. 10 cases study of EGFR inhibitors related skin rash with traditional Chinese drug regimen "San Liang San". *China Mod. Med.* **2009**, *16* (21), 66−68.
(22) Ritchie, M. E.; Phipson, B.; Wu, D.; Hu, Y. F.; Law, C. W.; Shi, W.; Smyth, G. K. *limma* powers differential expression analyses for RNA-sequencing and microarray studies. *Nucleic Acids Res.* **2015**, *43* (7), No. e47.
(23) Ma, H.; Yu, H.; Li, Z.; Cao, Z.; Du, Y.; Dai, J.; Zhi, D.; Xu, Y.; Li, N.; Wang, J. β-Carboline dimers inhibit the tumor proliferation by the cell cycle arrest of sarcoma through intercalating to Cyclin-A2. *Front. Immunol.* **2022**, *13*, No. 922183.
(24) Du, Y.; Ma, H.; Liu, Y.; Gong, R.; Lan, Y.; Zhao, J.; Liu, G.; Lu, Y.; Wang, S.; Jia, H.; Li, N.; Zhang, R.; Wang, J.; Sun, G. Major quality regulation network of flavonoid synthesis governing the bioactivity of black wolfberry. *New Phytol.* **2024**, *242* (2), 558−575.
(25) Du, Y.; Jia, H.; Yang, Z.; Wang, S.; Liu, Y.; Ma, H.; Liang, X.; Wang, B.; Zhu, M.; Meng, Y.; Gleason, M. L.; Hsiang, T.; Noorin, S.; Zhang, R.; Sun, G. Sufficient coumarin accumulation improves apple resistance to Cytospora mali under high-potassium status. *Plant Physiol.* **2023**, *192* (2), 1396−1419.
(26) Ciccia, F.; Rizzo, A.; Guggino, G.; Cavazza, A.; Alessandro, R.; Maugeri, R.; Cannizzaro, A.; Boiardi, L.; Iacopno, D. G.; Salvarani, C.; Triolo, G. Difference in the expression of IL-9 and IL-17 correlates with different histological pattern of vascular wall injury in giant cell arteritis. *Rheumatology* **2015**, *54* (9), 1596−1604.
(27) Thomas, L. S.; Targan, S. R.; Tsuda, M.; Yu, Q. T.; Salumbides, B. C.; Haritunians, T.; Mengesha, E.; McGovern, D. P. B.; Michelsen, K. S. The TNF family member TL1A induces IL-22 secretion in committed human T(h)17 cells via IL-9 induction. *J. Leukocyte Biol.* **2017**, *101* (3), 727−737.
(28) Aziz, K. E.; Wakefield, D. In vivo and in vitro expression of adhesion molecules by peripheral blood lymphocytes from patients with primary Sjogren's syndrome: Culture-associated enhancement of LECAM-1 and CD44. *Rheumatol. Int.* **1995**, *15* (2), 69−74.
(29) Pertovaara, M.; Silvennoinen, O.; Isomäki, P. STAT-5 is activated constitutively in T cells, B cells and monocytes from patients with primary Sjögren's syndrome. *Clin. Exp. Immunol.* **2015**, *181* (1), 29−38.
(30) Hernández-Molina, G.; Ruiz-Quintero, N.; Lima, G.; Hernández-Ramírez, D.; Llorente-Chávez, A.; Saavedra-González, V.; Jiménez-Soto, R.; Llorente, L. Chemokine tear levels in primary Sjögren's syndrome and their relationship with symptoms. *Int.. Ophthalmol.* **2022**, *42*, 2355−2361.
(31) Nath, S.; Mukherjee, P. MUC1: A multifaceted oncoprotein with a key role in cancer progression. *Trends Mol. Med.* **2014**, *20* (6), 332−342.
(32) Lee, J. S.; Lee, E. Y.; Ha, Y. J.; Kang, E. H.; Lee, Y. J.; Song, Y. W. Serum KL-6 levels reflect the severity of interstitial lung disease associated with connective tissue disease. *Arthritis Res. Ther.* **2019**, *21* (1), 58.
(33) Justet, A.; Neukirch, C.; Poubeau, P.; Arrault, X.; Borie, R.; Dombret, M. C.; Crestani, B. Successful rapid tocilizumab desensitization in a patient with Still disease. *J. Allergy Clin. Immunol.* **2014**, *2* (5), 631−632.
(34) Thompson, G.; Mclean-Tooke, A.; Wrobel, J.; Lavender, M.; Lucas, M. Sjögren syndrome with associated lymphocytic interstitial pneumonia successfully treated with tacrolimus and abatacept as an alternative to rituximab. *Chest* **2018**, *153* (3), e41−e43.
(35) Kuwahara, I.; JulianJ, E. P.; Hisatsune, A.; Lu, W. J.; Isohama, Y.; Miyata, T.; Kim, K. C. Neutrophil elastase stimulates MUC1 gene expression through increased Sp1 binding to the MUC1 promoter. *Am. J. Physiol.: Lung Cell. Mol. Physiol.* **2005**, *289*, L355−L362.
(36) Abate, W.; Alghaithy, A. A.; Parton, J.; Jones, K. P.; Jackson, S. K. Surfactant lipids regulate LPS-induced interleukin-8 production in A549 lung epithelial cells by inhibiting translocation of TLR4 into lipid raft domains. *J. Lipid Res.* **2010**, *51*, 334−344.
(37) Thirkill, T. L.; Cao, T.; Stout, M.; Blankenship, T. N.; Barakat, A.; Douglas, G. C. MUC1 is involved in trophoblast transendothelial migration. *Biochim. Biophys. Acta* **2007**, *1773*, 1007−1014.
(38) Yuan, Z. L.; Wong, S.; Borrelli, A.; Chung, M. A. Down-regulation of MUC1in cancer cells inhibits cell migration by promoting E-cadherin/catenin complex formation. *Biochem. Biophys. Res. Commun.* **2007**, *362*, 740−746.

https://doi.org/10.1021/acsomega.4c01147
ACS Omega 2024, 9, 30392−30403